

Theoretical aspects of W-pair production in e^+e^- collisions[†]

Stefan Dittmaier

*Fakultät für Physik, Universität Bielefeld,
Postfach 10 01 31, D-33501 Bielefeld, Germany*

Abstract

The most interesting theoretical features of W-pair production in e^+e^- collisions are reviewed. Based on an analysis of on-shell W-pairs, it is shown that the mere inclusion of leading $\mathcal{O}(\alpha)$ corrections—such as initial-state radiation, effects from the universal quantities $\Delta\alpha$ and Δr , and the Coulomb singularity—cannot be expected to approximate the $\mathcal{O}(\alpha)$ -corrected cross-section of $e^+e^- \rightarrow WW \rightarrow 4f$ to better than 1-2% for LEP2 energies. The importance of the gauge-invariance problem, arising from the introduction of finite decay widths, is discussed. The simplest consistent method to include $\mathcal{O}(\alpha)$ corrections at least to the doubly resonant contributions, viz. a pole expansion around the double resonance, is also briefly described.

October 1996

[†]Talk given at the 3rd *International Symposium on Radiative Corrections*, Cracow, Poland, August 1-5, 1996.

1 Introduction

LEP2 provides first experimental results on the process $e^+e^- \rightarrow WW \rightarrow 4f$ at center-of-mass (CMS) energies between 161 GeV and roughly 200 GeV. Future experiments at the next linear collider (NLC), which is planned for CMS energies of 0.5-2 TeV, will be able to explore higher energies.

The most prominent goal to be reached via W-pair production at LEP2 is a precise determination of the W-boson mass M_W . A reduction of the present experimental uncertainty of $\Delta M_W = 125 \text{ MeV}$ [1] by a factor of 3-4 is aimed at. The most promising methods for the extraction of M_W from the data are the investigation of the total cross-section near threshold and the reconstruction of M_W from the W-decay products, as extensively discussed in Ref. [2]. For the first method the total cross-section at $\sqrt{s} = 161 \text{ GeV}$, where the maximal sensitivity to M_W is reached, has to be known with an theoretical accuracy of 1-2% (half of the expected statistical error). The direct reconstruction relies on the invariant-mass distribution of the decay products which is strongly influenced by effects of initial-state radiation. Consequently, the inclusion of radiative corrections (RCs) in theoretical predictions is indispensable for both methods.

The second important issue accessible by $e^+e^- \rightarrow WW$ is the investigation of the triple-gauge-boson couplings. Although the non-abelian self-couplings of the Standard Model could be indirectly confirmed by the LEP1 observables and the W-boson mass via radiative corrections [3], only rather crude experimental bounds on the general (anomalous) structure of bosonic self-couplings exist, which result from hadron collisions. Although $e^+e^- \rightarrow WW$ is the first observable e^+e^- -process, where non-abelian self-couplings enter already lowest-order predictions, the sensitivity of the total cross-section to anomalous couplings at LEP2 energies is too weak to yield stringent bounds, and one is forced to inspect the angular distributions of the produced W bosons (see e.g. Ref. [4]). Since also RCs distort angular distributions, these mimic anomalous couplings and therefore have to be extracted. At NLC energies much more drastic effects of anomalous couplings can arise, but also RCs become more important.

The above considerations underline the importance of RCs to W-pair production, which are the subject of this short review. More detailed reviews can be found in Refs. [5, 6]. Following two steps of sophistication, we consider on-shell W-pairs in Sect. 2 before dealing with the complete four-fermion production process in Sect. 3. Section 4 contains our conclusions.

2 On-shell W-pair production

2.1 Born cross-section

We consider the reaction

$$e^+(p_+, \kappa_+) + e^-(p_-, \kappa_-) \rightarrow W^+(k_+, \lambda_+) + W^-(k_-, \lambda_-), \quad (1)$$

where p_\pm , k_\pm and κ_\pm , λ_\pm denote the momenta and helicities of the respective particles. The Mandelstam variables are defined by

$$s = 4E^2, \quad t = M_W^2 - 2E^2(1 - \beta \cos \theta), \quad (2)$$

where E is the beam energy, $\beta = \sqrt{1 - M_W^2/E^2}$ the W-boson velocity, and θ the scattering angle in the CMS. The lowest-order amplitude \mathcal{M}_B^κ gets contributions from the diagrams shown in Fig. 1 and reads

$$\mathcal{M}_B^\kappa = \frac{e^2}{2s_W^2} \frac{1}{t} \mathcal{M}_t^\kappa \delta_{\kappa-} + e^2 \left[\frac{1}{s} - \left(1 - \frac{1}{2s_W^2} \delta_{\kappa-} \right) \frac{1}{s - M_Z^2} \right] \mathcal{M}_s^\kappa, \quad (3)$$

where $\kappa = \pm$ is used as a shorthand for the electron helicity, which is conserved ($\kappa = \kappa_- = -\kappa_+$) since the electron mass m_e is neglected

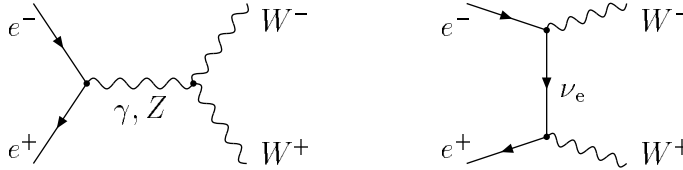


Figure 1: Born diagrams for $e^+e^- \rightarrow W^+W^-$.

whenever possible. We calculate in the on-shell scheme where the weak mixing angle is fixed by the ratio of gauge-boson masses, $c_w^2 = 1 - s_w^2 = M_W^2/M_Z^2$. The quantities \mathcal{M}_t^κ and \mathcal{M}_s^κ for the t - and s -channel graphs, respectively, contain the spinors and polarization vectors and depend on s , t , κ , and λ_\pm .

Near threshold ($\beta \rightarrow 0$) the s -channel contribution is suppressed by a factor β so that the t -channel contribution dominates, and the differential cross-section reads

$$\frac{d\sigma_B}{d\Omega} = \frac{\alpha^2}{4s_w^4} \frac{\beta}{s} \left[1 + 4\beta \cos\theta \frac{3c_w^2 - 1}{4c_w^2 - 1} + \mathcal{O}(\beta^2) \right]. \quad (4)$$

In the high-energy limit ($E \rightarrow \infty$) the total cross-section behaves as

$$\sigma_B = \frac{\pi\alpha^2}{4s_w^4} \frac{1}{s} \left[2 \log\left(\frac{s}{M_W^2}\right) - \frac{5}{2} - \frac{1}{3c_w^2} + \frac{5}{24c_w^4} + \mathcal{O}(\log s/s) \right]. \quad (5)$$

The presence of gauge cancellations between t - and s -channel contributions is necessary to guarantee unitarity for longitudinally polarized W bosons, i.e. the leading behavior of \mathcal{M}_t^κ and \mathcal{M}_s^κ is correlated. However, there is of course no high-energy relation between the contributions originating from the different gauge couplings, which lead to the following decomposition of \mathcal{M}_B^κ :

$$\mathcal{M}_B^\kappa = \frac{e^2}{2s_w^2} \mathcal{M}_I^\kappa \delta_{\kappa-} + e^2 \mathcal{M}_Q^\kappa. \quad (6)$$

\mathcal{M}_I^κ defines the “isospin part” with the associated coupling e/s_w , and \mathcal{M}_Q^κ the “electromagnetic part” with the coupling e .

2.2 Radiative corrections

The $\mathcal{O}(\alpha)$ RCs to the W-pair production cross-section consist of three different parts:

$$d\sigma = d\sigma_B(1 + \delta_V + \delta_S + \delta_H), \quad (7)$$

the virtual one-loop correction δ_V , the real soft-photon correction δ_S , and the hard bremsstrahlung correction δ_H . Both the complete virtual [7] and real [8] corrections were calculated by different groups.

The lowest-order and $\mathcal{O}(\alpha)$ -corrected total cross-sections are shown in Fig. 2, where here and in the following σ_B is parametrized by α , M_Z , M_W , and the input parameters are taken from Ref. [6]. The size of the relative RCs δ , which is also depicted in Fig. 2, is at the order of 5-10% for LEP2 energies. The large negative amount of δ near threshold indicates the necessity of soft-photon exponentiation in this region. For NLC energies the RCs are at the order of 20%, but we note that the RCs are further enhanced if the forward direction is excluded by an angular cut.

Concerning RCs the differences between W-pair and fermion-pair production at LEP2 and LEP1, respectively, are characterized by two features: Firstly, there is no simple effective Born approximation for W-pair production, and thus the RCs cannot be absorbed into effective couplings. Secondly, there is no gauge-invariant, unambiguous splitting between QED and genuinely weak corrections for W pairs. Moreover, the analytical structure of the RCs is involved resulting in long and rather slow computer codes.

A first step towards a successful approximation of the RCs is to control the leading corrections, which are of the following origin:

(i) Initial-state radiation:

Collinear initial-state radiation (ISR) off the incoming electrons and positrons yield large corrections of $\mathcal{O}(\alpha^n \log^n m_e^2/Q^2)$ with $n = 1, 2, \dots$. The leading logarithms are universal and can be most easily calculated via the structure-function approach [9]:

$$\delta\sigma_{\text{ISR}}(s) = \int_{4M_W^2/s}^1 dx \Phi(x, Q^2) \sigma_B(xs), \quad (8)$$

i.e. by a convolution of the lowest-order cross-section with a flux function Φ . In $\mathcal{O}(\alpha)$ the flux function reads

$$\begin{aligned} \Phi(x, Q^2) = \frac{\alpha}{\pi} \log\left(\frac{Q^2}{m_e^2}\right) & \left[\delta(1-x) \left(\frac{3}{2} + 2 \log \frac{\Delta E}{E} \right) \right. \\ & \left. + \theta\left(1 - \log \frac{\Delta E}{E} - x\right) \frac{1+x^2}{1-x} \right] + \mathcal{O}(\alpha^2), \end{aligned} \quad (9)$$

but Φ is also known up to $\mathcal{O}(\alpha^3 \log^3 m_e^2/Q^2)$ (see Ref. [6] and references therein). The soft-photon cutoff ΔE , which drops out in

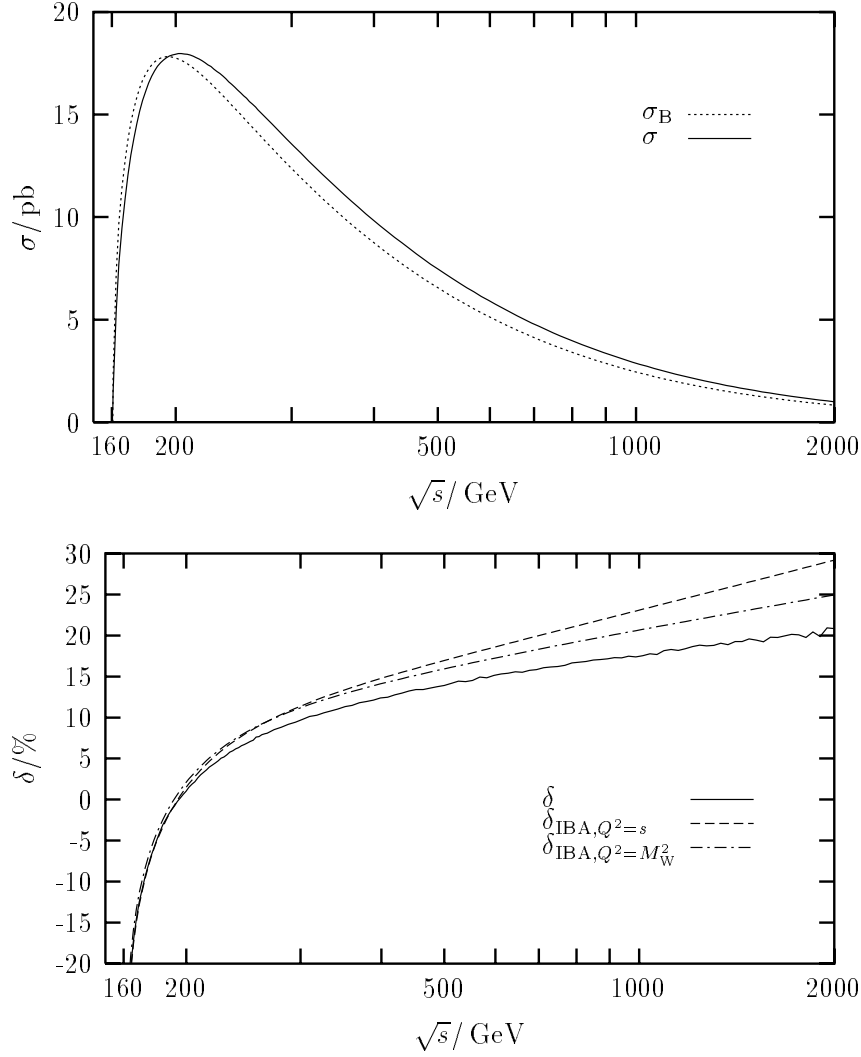


Figure 2: Born cross-section σ_B , $\mathcal{O}(\alpha)$ -corrected cross-section (including also leading higher-order effects via $\Delta\alpha$ and Δr) $\sigma = \sigma_B(1 + \delta)$, and relative correction δ for unpolarized particles. The improved Born approximation (IBA) of (12) is also shown for two different choices of the photon splitting scale Q^2 .

the final result, separates the contributions of soft ($E_\gamma < \Delta E$) and hard ($E_\gamma > \Delta E$) photons. The splitting scale Q^2 is not determined in leading logarithmic approximation and thus expresses part of the theoretical uncertainty owing to neglected non-leading corrections. At LEP2 energies ISR corrections amount to roughly 6%.

(ii) Running of the electromagnetic coupling $\alpha(q^2)$:

The definition of the $ee\gamma$ coupling e in the low-energy limit (Thomson scattering) leads to large universal corrections to processes which involve energies at the electroweak scale. These corrections, which are of $\mathcal{O}(\alpha^n \log^n m_f^2/q^2)$ for light fermions f , can be accounted for by introducing the running electromagnetic coupling $\alpha(q^2)$, which replaces the fine-structure constant $\alpha(0) = e^2/4\pi = 1/137.0\dots$ as input parameter. In perturbation theory $\alpha(q^2)$ is parametrized by $\alpha(0)$ and the light fermion masses m_f where the quark masses are adjusted to reproduce the hadronic vacuum polarization [10]. At LEP2 energies the transition from $\alpha(0)$ to $\alpha(q^2)$ corrects the cross-section by about 8%.

(iii) Coulomb singularity:

Near threshold the long range of the Coulomb interaction between slowly moving W bosons causes large universal corrections, which are proportional to the Born cross-section,

$$\delta\sigma_{\text{Coul}} \underset{\beta \rightarrow 0}{\sim} \frac{\alpha\pi}{2\beta} \sigma_{\text{B}}. \quad (10)$$

The singular behavior of the relative correction at $\beta \rightarrow 0$ is a peculiarity of the on-shell approximation, which assumes stable W bosons. This singularity is regularized by a finite W decay width, since the range of interaction is effectively truncated by the W decay (see next section).

(iv) Effects from light or heavy masses:

In analogy to the long-range effect of the Coulomb interaction, which is due to the exchange of massless photons, the exchange of

a relatively light Higgs boson between slowly moving W bosons near threshold leads to a Yukawa-like interaction. In the limit $M_H \ll M_W$ the leading behavior is given by

$$\delta\sigma_{\text{LH}} \xrightarrow{M_H \rightarrow 0} \frac{\alpha}{2s_W^2} \frac{M_W}{M_H} \sigma_B, \quad (11)$$

but also more sophisticated approximations are known [11]. For $M_H \sim 60\text{--}300\text{ GeV}$ this effect influences the cross-section about 1% at threshold, but the effect becomes negligible for higher values of M_H and E .

In the large-mass limit [12] for M_H and the top-quark mass m_t one gets leading corrections proportional to $\alpha \log M_H$, $\alpha \log m_t$, and $\alpha m_t^2/M_W^2$, where the m_t^2 correction only enters the isospin part, as specified in (6). In the isospin part, which dominates at low energies, all above-mentioned leading heavy-mass corrections enter via the renormalization of s_W , i.e. are identical to the ones in the well-known quantity Δr , and thus can be absorbed by the substitution $e^2/s_W^2 \rightarrow 4\sqrt{2}G_\mu M_W^2$. Here G_μ is introduced as input parameter, and M_W is calculated from muon decay. The heavy-mass correction to the electromagnetic part yield contributions of about 0.1% at LEP2 energies and are thus negligible.

2.3 Approximations for radiative corrections

Taking into account the most important leading corrections, we arrive at the following improved Born approximation (IBA)

$$\begin{aligned} \left(\frac{d\sigma}{d\Omega}\right)_{\text{IBA}} &= \frac{\beta}{64\pi^2 s} \left| 2\sqrt{2}G_\mu M_W^2 \mathcal{M}_I^\kappa \delta_{\kappa-} + 4\pi\alpha(s) \mathcal{M}_Q^\kappa \right|^2 \\ &+ \left(\frac{d\sigma}{d\Omega}\right)_{\text{ISR}} + \left(\frac{d\sigma}{d\Omega}\right)_{\text{Coul}} (1 - \beta^2)^2, \end{aligned} \quad (12)$$

as proposed in Ref. [12]. Here the Coulomb correction is accompanied by the weight function $(1 - \beta^2)^2$, which switches this effect off for $\beta \rightarrow 1$. Figure 2 shows the comparison of the exact $\mathcal{O}(\alpha)$ correction δ (+ leading higher-order effects via $\Delta\alpha$ and Δr) to the total unpolarized

cross-section with the IBA for two different choices of the ISR splitting scale Q^2 . We recall that the complete bremsstrahlung spectrum is included in δ in this figure. In Tab. 1 we further illustrate the quality of the IBA (with $Q^2 = s$) by giving its deviation Δ_{IBA} from δ for different scattering angles θ using the soft-photon approximation, i.e. excluding hard photons with $E_\gamma > \Delta E$ but adding the exact ΔE terms of the soft-photon correction to the IBA. For LEP2 energies we read off an accuracy of 1-2%. Although the IBA remains still valid within $\lesssim 5\%$ in the forward direction, $\theta \lesssim 5^\circ$, up energies of 2 TeV, the IBA is not able to reproduce the angular distribution of the cross-section in reasonable approximation for NLC energies.

In addition to the IBA Tab. 1 also shows a kind of form-factor approximation (FFA) [12] for the one-loop matrix element:

$$\mathcal{M}_{\text{FFA}}^\kappa = F_I^\kappa(s, t) \mathcal{M}_I^\kappa + F_Q^\kappa(s, t) \mathcal{M}_Q^\kappa. \quad (13)$$

The four form-factors $F_{I,Q}^\kappa(s, t)$ have been extracted from the exact one-loop result (which consists of twelve independent ones) by inspecting the structure of the corrections to the different helicity amplitudes¹. Obviously (13) includes all leading and non-leading corrections associated with the Born structure. The FFA is excellent whenever the cross-section is sizable. More precisely, in general it approximates the $\mathcal{O}(\alpha)$ -corrected cross-section within $\sim 0.1\%$, and even at the per-cent level if the Born cross-section is suppressed. Although this FFA demonstrates that the Born structure indeed dominates also the one-loop RCs, its evaluation is practically as complicated as the exact one-loop calculation, which limits its practical use.

For energies above 500 GeV a relatively simple approximation of the virtual and soft-photon $\mathcal{O}(\alpha)$ corrections exists [14] which was constructed by a systematic asymptotic expansion for $E \gg M_W$. The leading corrections are of the form $\alpha \log(q_1^2/M_W^2) \log(q_2^2/M_W^2)$ with $q_i^2 = s, t, u$ and originate from vertex and box graphs. Depending on the hierarchy of scales the heavy-mass effects in longitudinal W-boson production can be additionally enhanced: for $s \gg m_t^2, M_H^2 \gg M_W^2$

¹A similar form-factor approximation was proposed in Ref. [13], where the structure of anomalous couplings was used as guideline.

\sqrt{s}/GeV	θ	$\sigma_{\text{B}}/\text{fb}$	$\Delta_{\text{IBA}}/\%$	$\Delta_{\text{FFA}}/\%$	$\Delta_{\text{HEA}}/\%$
161	$(10^\circ, 170^\circ)$	3753.2	1.5	0.00	37
	10°	367.0	1.6	0.00	36
	90°	300.7	1.4	0.00	37
	170°	250.0	1.3	0.00	37
175	$(10^\circ, 170^\circ)$	15591	1.3	0.03	12
	10°	3380	1.7	0.00	10
	90°	1001	1.0	0.05	12
	170°	439	0.59	0.00	12
200	$(10^\circ, 170^\circ)$	17107	1.5	0.01	3.7
	10°	6463	1.8	0.00	2.3
	90°	812	1.4	0.02	4.7
	170°	255	1.3	0.00	3.8
500	$(10^\circ, 170^\circ)$	4413.1	4.7	-0.06	-0.85
	10°	11604.4	1.9	0.00	-0.67
	90°	75.4	10	-0.29	-0.05
	170°	6.5	14	-0.19	3.5
1000	$(10^\circ, 170^\circ)$	1084.3	11	0.06	0.21
	10°	3292.3	3.9	0.00	1.1
	90°	16.7	23	0.08	0.54
	170°	0.6	28	-0.77	6.4
2000	$(10^\circ, 170^\circ)$	267.57	22	0.12	0.17
	10°	823.35	9.7	0.02	0.64
	90°	4.03	39	-0.16	0.34
	170°	0.09	46	-2.3	5.4

Table 1: Unpolarized Born cross-section σ_{B} and differences Δ (normalized to σ_{B}) between various approximations and exact calculation of the one-loop RCs for different CMS energies and angles, where $(10^\circ, 170^\circ)$ denotes the angular interval for integrated cross-sections.

power corrections of $\mathcal{O}(\alpha m_t^2/M_W^2)$ and $\mathcal{O}(\alpha M_H^2/M_W^2)$ show up (incomplete screening); for $m_t^2, M_H^2 \gg s \gg M_W^2$ one observes so-called delayed unitarity effects leading to terms of $\mathcal{O}(\alpha s/M_W^2 \log m_t)$ and $\mathcal{O}(\alpha s/M_W^2 \log M_H)$. By construction the high-energy approximation (HEA) asymptotically approaches the exact one-loop RCs, but already for energies of 500-1000 GeV the deviation is only of the order of 1% for small and intermediate scattering angles, as can be read off from Tab. 1.

3 Four-fermion production

3.1 Born cross-section and its complications

The simplest extension of on-shell W-pair production to the off-shell case consists in the convolution

$$\sigma(s) = B_{f_1 \bar{f}_2} B_{f_3 \bar{f}_4} \int dk_+^2 \rho_W(k_+^2) \int dk_-^2 \rho_W(k_-^2) \sigma_{eeWW}(s, k_+^2, k_-^2), \quad (14)$$

of the “off-shell cross-section” σ_{eeWW} with the Breit-Wigner distribution

$$\rho_W(k_\pm^2) = \frac{1}{\pi} \frac{M_W \Gamma_W}{|k_\pm^2 - M_W^2 + i M_W \Gamma_W|^2} \xrightarrow{\Gamma_W \rightarrow 0} \delta(k_\pm^2 - M_W^2), \quad (15)$$

as proposed in Ref. [15]. Here Γ_W denotes the decay width of the W boson, and $B_{f_i \bar{f}_j}$ the branching ratio for $W \rightarrow f_i \bar{f}_j$. For $\Gamma_W \rightarrow 0$ one clearly obtains the narrow-width approximation. Obviously this approach does not lead to gauge-invariant results for two reasons: Firstly, not all diagrams for the process $e^+e^- \rightarrow f_1 \bar{f}_2 f_3 \bar{f}_4$ are taken into account, but only the doubly resonant ones which factorize into production and decay. Secondly, the inclusion of finite-width effects goes beyond a pure perturbative expansion and deserves particular care.

The first problem can in principle be solved by taking into account all tree graphs contributing to $e^+e^- \rightarrow f_1 \bar{f}_2 f_3 \bar{f}_4$ which includes in addition so-called “background diagrams” with only one or even no resonant W boson. Figure 3 shows some typical topologies for such graphs at tree level. The number of background diagrams depends

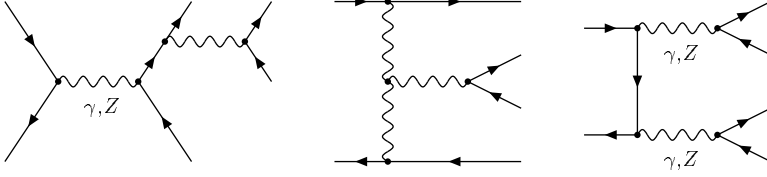


Figure 3: Typical topologies for background graphs to $e^+e^- \rightarrow WW \rightarrow f_1\bar{f}_2f_3\bar{f}_4$ at tree level.

on the final state, ranging from 6 for $e^+e^- \rightarrow \mu^-\bar{\nu}_\mu\tau^+\nu_\tau$ to 53 for $e^+e^- \rightarrow e^+\nu_e e^-\bar{\nu}_e$. The numerical impact of these graphs in general is of $\mathcal{O}(\Gamma_W/M_W) \sim 3\%$ relative to the doubly resonant contributions and can be reduced by invariant-mass cuts

$$M_W - \Delta_W < M_{f_1\bar{f}_2}, M_{f_3\bar{f}_4} < M_W + \Delta_W \quad (16)$$

by a factor of Δ_W/M_W , where $M_{f_i\bar{f}_j}$ is the invariant mass of the corresponding fermion pair. However, in this context it should be mentioned that the influence of the background diagrams can be enhanced in certain regions of phase space such as for forward e^\pm scattering. The numerical evaluation of cross-sections including this background has been performed by several authors using Monte-Carlo or semianalytical methods and is reviewed elsewhere [16] (see also Ref. [17]).

The second problem mentioned above is seen by inspecting the general structure of the amplitude,

$$\mathcal{M} = \frac{R_{+-}(k_+^2, k_-^2)}{(k_+^2 - M_W^2)(k_-^2 - M_W^2)} + \frac{R_+(k_+^2, k_-^2)}{k_+^2 - M_W^2} + \frac{R_-(k_+^2, k_-^2)}{k_-^2 - M_W^2} + N(k_+^2, k_-^2), \quad (17)$$

which contains the doubly, singly, and non-resonant contributions R_{+-} , R_\pm , and N , respectively. Gauge invariance implies that \mathcal{M} does not depend on the gauge-fixing procedure of the perturbative calculation (usually quantified by a gauge parameter) and that \mathcal{M} obeys Ward identities which guarantee gauge cancellations and thus unitarity. However, this is only the case for the sum but not for the single

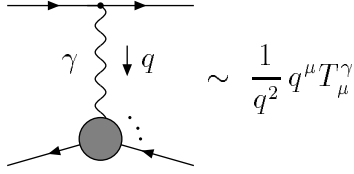


Fig. 4a)

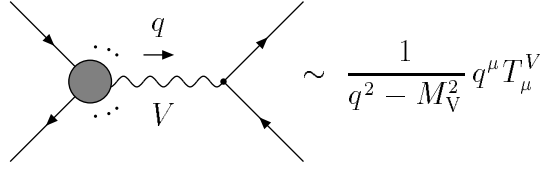


Fig. 4b)

Figure 4: Typical situations for gauge cancellations for a) $|q^2| \ll s$ due to electromagnetic gauge invariance, and for b) $q^0 \gg M_V$ due to SU(2) gauge invariance.

terms in (17). Therefore, introducing a (possibly running) finite width via

$$\frac{1}{k_{\pm}^2 - M_W^2} \rightarrow \frac{1}{k_{\pm}^2 - M_W^2 + iM_W\Gamma_W(k_{\pm}^2)} \quad (18)$$

breaks gauge invariance by terms which are formally of $\mathcal{O}(\Gamma_W/M_W)$ [18]. However, these gauge-invariance-breaking terms can be further enhanced in the presence of small scales or if gauge cancellations are disturbed. Gauge cancellations are required for a well-behaved matrix element if external fermionic currents $\bar{u}(p)\gamma^\mu u'(p')$ become proportional to the momentum q^μ of the gauge boson which directly couples to this current. Figure 4 shows typical situations where gauge cancellations are relevant: Figure 4a) illustrates that $q^\mu T_\mu^\gamma$ must compensate the pole $1/q^2$ in the photon propagator for forward electron scattering ($|q^2| \ll s$). Figure 4b) shows the production of an effectively longitudinally polarized massive gauge boson V at high energies ($q^0 \gg M_V$) where cancellations in $q^\mu T_\mu^V$ are necessary in order to guarantee unitarity. These cancellations are ruled by the Ward identities

$$q^\mu T_\mu^\gamma = 0, \quad q^\mu T_\mu^Z = iM_Z T^\chi, \quad q^\mu T_\mu^{W^\pm} = \pm M_W T^{\phi^\pm}, \quad (19)$$

where the first one expresses electromagnetic current conservation, and the others imply the Goldstone-boson equivalence theorem, which relates the amplitudes for Z and W bosons to the ones for their respective would-be Goldstone bosons χ and ϕ .

In the literature several methods for the introduction of finite decay widths in amplitudes were proposed which are discussed in view of the above gauge-invariance issue elsewhere [19]. Here we just mention the field-theoretically most convincing approach of the so-called fermion-loop scheme [20], which consists of the consequent inclusion of all fermionic one-loop corrections (self-energy, vertex and box corrections) to tree-level amplitudes using Dyson-resummed propagators. This approach is manifestly gauge-parameter-independent, preserves the crucial Ward identities (19), and introduces the complete finite-width effects of unstable particles that decay exclusively into fermion pairs, such as the weak gauge bosons Z and W.

3.2 Radiative corrections

Owing to its complexity a complete calculation of the $\mathcal{O}(\alpha)$ RCs to four-fermion production has not been presented yet, and hopefully is not needed. So far only leading RCs have been included in theoretical predictions.

For on-shell W-pair production we have seen in the last section that leading-log ISR, leading electroweak corrections in G_μ and $\alpha(q^2)$, and Coulomb correction approximate the complete $\mathcal{O}(\alpha)$ -corrected cross-section within 1-2% at LEP2 energies. Therefore we expect that this is also the typical theoretical uncertainty in the corresponding leading-log improved predictions for four-fermion production, at least in regions of phase space where the doubly resonant graphs are dominant. In practice ISR is treated either using the structure-function approach analogously to (8) or using parton-shower methods (see e.g. Refs. [6, 17] for details). Moreover, the absorption of the leading weak corrections arising from renormalization ($\Delta\alpha$, Δr) follows exactly the same lines as in the on-shell case. However, the Coulomb correction is considerably modified by finite-width effects [21]. The singular β^{-1} correction factor to the on-shell cross-section is regularized in the off-shell case:

$$\delta\sigma_{\text{Coul}} = \sigma_{\text{B},2\text{-res}} \frac{\alpha\pi}{2\bar{\beta}} \left[1 - \frac{2}{\pi} \arctan \left(\frac{|\beta_{\text{M}}|^2 - \bar{\beta}^2}{2\bar{\beta} \text{Im} \beta_{\text{M}}} \right) \right], \quad (20)$$

with $\sigma_{\text{B},2\text{-res}}$ denoting the doubly resonant part of the Born cross-section, and

$$\begin{aligned}\bar{\beta} &= \sqrt{1 - 2(k_+^2 + k_-^2)/s + (k_+^2 - k_-^2)^2/s^2}, \\ \beta_M &= \sqrt{1 - 4(M_W^2 - iM_W\Gamma_W)/s}.\end{aligned}\tag{21}$$

The on-shell singularity is recovered by taking $\Gamma_W \rightarrow 0$ after setting $\bar{\beta}^2 = \text{Re } \beta_M^2 = \beta^2$. For finite Γ_W the $\bar{\beta}^{-1}$ correction is screened if the average velocity $\bar{\beta}$ becomes smaller than $|\beta_M| \gtrsim \sqrt{\Gamma_W/M_W}$. The maximal effect of $\sim 6\%$ is reached at threshold, while this correction still amounts to 2-3% for CMS energies around $\sqrt{s} \sim 175 \text{ GeV}$.

The approximation of RCs that includes only the leading effects described above is certainly not able to match the aimed experimental 1% accuracy. Therefore at least the $\mathcal{O}(\alpha)$ corrections to the doubly resonant contributions have to be taken into account. A first step towards this direction is reached if finite decay widths are introduced via the fermion-loop scheme, as briefly described in the previous subsection. In this approach the complete fermion-loop corrections of $\mathcal{O}(\alpha)$ are included which represent a substantial part of the complete $\mathcal{O}(\alpha)$ RCs. Although there is a natural generalization of the gauge-invariant fermion-loop resummation to the complete (fermionic + bosonic) RCs within the background-field method [22], the general problem is not yet under control. On the one hand, gauge invariance, which guarantees the Ward identities (19), requires the inclusion of all (doubly, singly, and non-resonant) $\mathcal{O}(\alpha)$ RCs; on the other hand, a gauge-parameter dependence remains at the loop order that is incomplete, e.g. in $\mathcal{O}(\alpha^2)$ in a complete Dyson-resummed one-loop calculation. This direction certainly deserves further investigations.

For a first approach to include also bosonic $\mathcal{O}(\alpha)$ RCs one can perform a pole expansion [23] about the double resonance and keep only the doubly resonant terms, which are known to be gauge-independent. Although the reliability of this approach near threshold is not clear, the relative uncertainty for energies of $\sqrt{s} \gtrsim 175 \text{ GeV}$ is expected to be of order $(\alpha/\pi)(\Gamma_W/M_W)\mathcal{O}(1) \lesssim 0.1\%$. Technically the pole-scheme calculation consists in taking only the contribution of $R_{+-}(k_+^2, k_-^2)$ in the matrix element, as specified in (17), by setting $k_\pm^2 = M_W^2$ in R_{+-} .

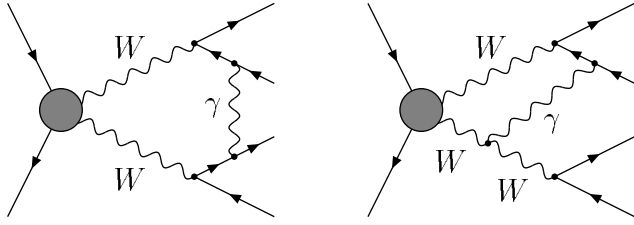


Figure 5: Examples for non-factorizable photonic corrections.

This procedure considerably reduces the number of relevant diagrams but includes the complete $\mathcal{O}(\alpha)$ RCs to the on-shell production and the subsequent decay of the W bosons. Additionally doubly resonant, but non-factorizable diagrams contribute, which arise from photonic initial-final and final-final state interactions, as indicated in Fig. 5. It turns out that only infrared photons are relevant for the doubly resonant part. In a special kind of soft-photon approximation it was shown in Ref. [24] that the doubly resonant virtual + soft-photonic $\mathcal{O}(\alpha)$ contributions to the total cross-section cancel. In the same approximation this kind of correction was calculated in Ref. [25] for the differential cross-section, where non-vanishing corrections to the invariant-mass distributions occur. Unfortunately a complete numerical evaluation of $e^+e^- \rightarrow WW \rightarrow 4f$ in the pole scheme has not yet been presented in the literature.

4 Conclusions

We have reviewed theoretical aspects of W-pair production in e^+e^- annihilation by placing the emphasis on $\mathcal{O}(\alpha)$ RCs. The dominant $\mathcal{O}(\alpha)$ RCs are of universal origin, viz. collinear ISR, renormalization effects due to $\Delta\alpha$ and Δr , and the Coulomb singularity near threshold. They are also known for the four-fermion production process $e^+e^- \rightarrow 4f$ and thus can be easily included in present-day Monte-Carlo event generators. However, a comparison of these dominant RCs with exact $\mathcal{O}(\alpha)$ calculations for on-shell W-pair production reveals that for typical LEP2 energies one cannot expect to approximate

the full $\mathcal{O}(\alpha)$ -corrected cross-section for $e^+e^- \rightarrow 4f$ to better than 1-2% by including only these leading effects. Thus, also non-leading $\mathcal{O}(\alpha)$ corrections have to be taken into account to match the aimed experimental error of roughly 1% at LEP2.

The introduction of finite decay widths of resonating particles in amplitudes is non-trivial owing to problems with gauge invariance. At tree level a convincing solution exists for gauge-boson resonances, however, the general problem requires further investigations. A first approximation for the inclusion of $\mathcal{O}(\alpha)$ RCs to $e^+e^- \rightarrow WW \rightarrow 4f$ can be obtained via a pole expansion about the double resonance and keeping only the doubly resonant contributions. This procedure includes all $\mathcal{O}(\alpha)$ RCs to the on-shell W-pair production and the W decay, but also some non-factorizable photonic corrections arising from initial-final and final-final state interactions.

In this short review we could not consider final-state interactions which are associated with hadronization, such as color reconnection and Bose-Einstein correlations, which both influence the W-boson mass determination at LEP2. For these effects we refer to the literature (see Ref. [2] and references therein).

Acknowledgements

The author would like to thank the organizers for the kind invitation and for providing a very warm atmosphere during the conference. A. Denner is also gratefully acknowledged for helpful discussions.

References

- [1] UA2 Collaboration: J.Alitti et al, *Phys.Lett.* **B276** (1992) 354;
 CDF Collaboration: F.Abe et al, *Phys.Rev.Lett.* **65** (1990) 2243, *Phys.Rev.* **D43** (1991) 2070, *Phys.Rev.* **D52** (1995) 4784, *Phys.Rev.Lett.* **75** (1995) 11;
 DØ Collaboration: S.Abachi et al, preliminary result presented by U.Heintz, Les Rencontres de Physique de la Vallee d'Aoste, La Thuile, March 1996.

- [2] Z.Kunszt et al, in *Physics at LEP2*, eds. G.Altarelli, T.Sjöstrand, F.Zwirner, CERN 96-01, Vol.1, p.141, hep-ph/9602352.
- [3] S.Dittmaier, K.Kolodziej, M.Kuroda, D.Schildknecht, *Nucl.Phys.* **B426** (1994) 249, E: **B446** (1995) 334;
P.Gambino, A.Sirlin, *Phys.Rev.Lett.* **73** (1994) 621;
Z.Hioki, *Phys.Lett.* **B340** (1994) 181;
F.Jegerlehner, *Nucl.Phys. B (Proc.Suppl.)* **37B** (1994) 129.
- [4] G.Gounaris et al, in *Physics at LEP2*, eds. G.Altarelli, T.Sjöstrand, F.Zwirner, CERN 96-01, Vol.1, p.525, hep-ph/9601233.
- [5] W.Beenakker, A.Denner, *Int.J.Mod.Phys.* **A9** (1994) 4837.
- [6] W.Beenakker et al, in *Physics at LEP2*, eds. G.Altarelli, T.Sjöstrand, F.Zwirner, CERN 96-01, Vol.1, p.79, hep-ph/9602351.
- [7] M.Böhm et al, *Nucl.Phys.* **B304** (1988) 463;
J.Fleischer, F.Jegerlehner, M.Zralek, *Z.Phys.* **C42** (1989) 409.
- [8] V.Barger, T.Han, R.J.N.Phillips, *Phys.Rev.* **D39** (1989) 146;
W.Beenakker, K.Kolodziej, T.Sack, *Phys.Lett.* **B258** (1991) 469;
W.Beenakker, F.A.Berends, T.Sack, *Nucl.Phys.* **B367** (1991) 287;
K.Kolodziej, M.Zralek, *Phys.Rev.* **D43** (1991) 3619;
H.Tanaka, T.Kaneko, Y.Shimizu, *Comp.Phys.Comm.* **64** (1991) 149;
E.N.Argyres, O.Korakianitis, C.G.Papadopoulos, W.J.Stirling, *Phys.Lett.* **B259** (1991) 195;
J.Fleischer, F.Jegerlehner, K.Kolodziej, *Phys.Rev.* **D47** (1993) 830.
- [9] W.Beenakker, F.A.Berends, W.L.v.Neerven, in *Radiative Corrections for e^+e^- Collisions*, ed. J.H.Kühn (Springer, Berlin, 1989), p.3.
- [10] H.Burkhardt, B.Pietrzyk, *Phys.Lett.* **B356** (1995) 398;
S.Eidelman, F.Jegerlehner, *Z.Phys.* **C67** (1995) 585.

- [11] W.Beenakker, G.J.v.Oldenborgh, *Phys.Lett.* **B381** (1996) 248.
- [12] M.Böhm, A.Denner, S.Dittmaier, *Nucl.Phys.* **B376** (1992) 29; E: **B391** (1993) 483.
- [13] J.Fleischer et al, *Nucl.Phys.* **B378** (1992) 443, E: **B426** (1994) 246.
- [14] W.Beenakker et al, *Phys.Lett.* **B317** (1993) 622; *Nucl.Phys.* **B410** (1993) 245.
- [15] T.Muta, R.Najima, S.Wakaizumi, *Mod.Phys.Lett.* **A1** (1986) 203.
- [16] T.Ohl, these proceedings.
- [17] D.Bardin et al, in *Physics at LEP2*, eds. G.Altarelli, T.Sjöstrand, F.Zwirner, CERN 96-01, Vol.2, p.3, hep-ph/9602393.
- [18] A.Aeppli, F.Cuyper, G.J.v.Oldenborgh, *Phys.Lett.* **B314** (1993) 413.
- [19] W.Beenakker, these proceedings.
- [20] E.N.Argyres et al, *Phys.Lett.* **B358** (1995) 339;
W.Beenakker et al, in preparation.
- [21] V.S.Fadin, V.A.Khoze, A.D.Martin, *Phys.Lett.* **B311** (1993) 311;
D.Bardin, W.Beenakker, A.Denner, *Phys.Lett.* **B317** (1993) 213;
A.Chapovsky, V.S.Fadin, V.A.Khoze, A.D.Martin, *Phys.Rev.* **D52** (1995) 1377.
- [22] A.Denner, S.Dittmaier, G.Weiglein, *Nucl.Phys.* **B440** (1995) 95;
A.Denner, S.Dittmaier, *Phys.Rev.* **D54** (1996) 4499.
- [23] M.Veltman, *Physica* **29** (1963) 186;
R.G.Stuart, *Phys.Lett.* **B262** (1991) 113;
A.Aeppli, G.J.v.Oldenborgh, D.Wyler, *Nucl.Phys.* **B428** (1994) 126.
- [24] V.S.Fadin, V.A.Khoze, A.D.Martin, *Phys.Rev.* **D49** (1994) 2247.
- [25] K.Melnikov, O.Yakovlev, *Nucl.Phys.* **B471** (1996) 90.